PROCEEDINGS OF SCIENCE

LHCb overview

Émilie Maurice[*†]
LAL, Université Paris-Sud, CNRS/IN2P3, Orsay, France
also at LLR, École polytechnique, CNRS/IN2P3, Palaiseau, France
E-mail: emilie.maurice@llr.in2p3.fr

The LHCb detector, with its excellent momentum resolution and particle identification, is ideally suited for measuring heavy-quark hadron and quarkonium production properties. Recent LHCb measurements in heavy-ion collisions, including the fixed-target configuration, are presented.

International Conference on Hard and Electromagnetic Probes of High-Energy Nuclear Collisions
30 September - 5 October 2018
Aix-Les-Bains, Savoie, France

[*]Speaker.
[†]on behalf of the LHCb collaboration

PoS(HardProbes2018)008

1. Introduction

At high energy densities, a hot and dense medium of deconfined quarks and gluons, called Quark-Gluon Plasma (QGP) is produced. This new state of matter is studied in ultra-relativistic heavy-ion collisions, where heavy quarks are crucial probes. Produced via hard interactions at the early stage of the nucleus-nucleus collisions, before the QGP formation, heavy quarks experience the entire evolution of the QGP. A correct interpretation of these probes requires a full understanding of the Cold Nuclear Matter (CNM) effects, which are present regardless of the formation of the deconfined medium. To disentangle the CNM effects from the genuine QGP effects, heavy-flavor production in proton-nucleus collisions have to be studied. In this report, we present the recent heavy-ion results on heavy-flavor production in proton-lead, lead-lead and fixed-target collisions collected by the LHCb detector.

2. The LHCb detector

The LHCb detector [1] is a single-arm forward spectrometer covering the pseudorapidity range $2 < \eta < 5$. The LHCb experiment was designed for precision measurements in the b and c quark sectors, but it is also a general purpose detector. The detector, consisting of tracking systems, hadron-particle identification, calorimeters and muon system, is fully instrumented in the fiducial region. Thanks to this unique feature, LHCb studies heavy flavors in a unique kinematic region: low transverse momentum p_T, large rapidity y, complementary to other LHC experiments.

The LHCb experiment has collected data of proton-proton (pp), proton-lead (pPb) and lead-lead (PbPb) collisions. Since the LHCb detector covers only one direction of the full acceptance, there are two distinctive beam configurations for the pPb collisions. In the forward (backward) configuration, the proton (lead) beam enters LHCb detector from the interaction point. The proton beam and the lead beam have different energies per nucleon in the laboratory frame, so the nucleon-nucleon center-of-mass frame is boosted in the proton direction with a rapidity shift. Therefore the LHCb acceptance for the forward configuration is $1.5 < y^* < 4$, and for the backward is $-5 < y^* < -2.5$.

On top of that, LHCb provides the unique capability at the LHC to collect fixed-target collisions thanks to the System for Measuring the Overlap with Gas (SMOG) [2]. Originally designed for precise luminosity measurements, SMOG allows to inject noble gas such as argon or helium inside the primary LHC vacuum around the LHCb vertex detector (VELO). Since 2015, LHCb has started to exploit SMOG to perform physics runs, using special fills not devoted to pp physics, with different beam (p or Pb) and target configurations, allowing unique production studies which are relevant to cosmic ray and heavy-ion physics.

3. Fixed-target

At the LHC energy scale, a large amount of charmonium is produced in nucleus-nucleus collisions, leading to a competition between the charmonium suppression due to the color screening [3] and the charmonium enhancement due to the recombination mechanism [4], increasing the complexity of the results interpretation. Therefore the study of the charmonium suppression is ideal

at lower centre-of-mass energy of $\sqrt{s_{NN}} \sim 100$ GeV, to avoid any statistical recombination. For those studies, the LHCb fixed-target configuration is optimal, producing proton-nucleus (nucleus-nucleus) collisions with $\sqrt{s_{NN}}$ between 69 and 115 GeV.

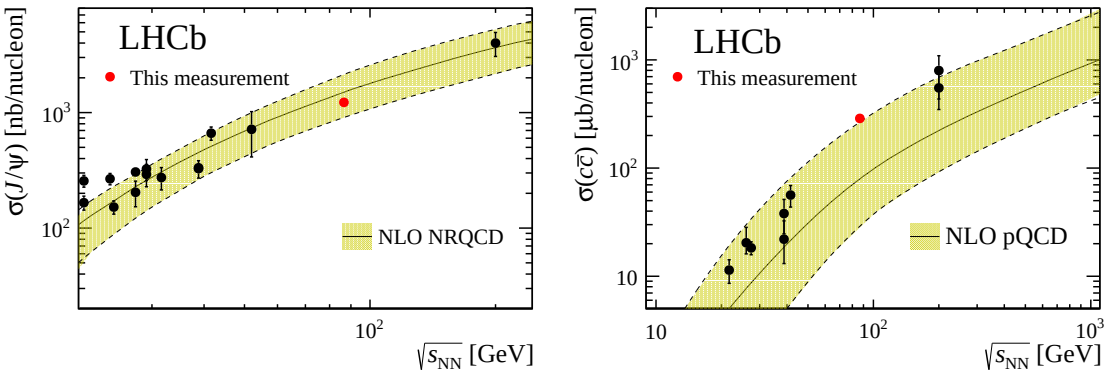

Figure 1: J/ψ (left) and $c\bar{c}$ (right) cross-section measurements as a function of the centre-of-mass energy compared with other experimental data (represented by black points). The band corresponds to a fit based on NLO NRQCD calculations for J/ψ [38] and NLO pQCD calculations for $c\bar{c}$ as a function of the centre-of-mass energy. More details are given in [5].

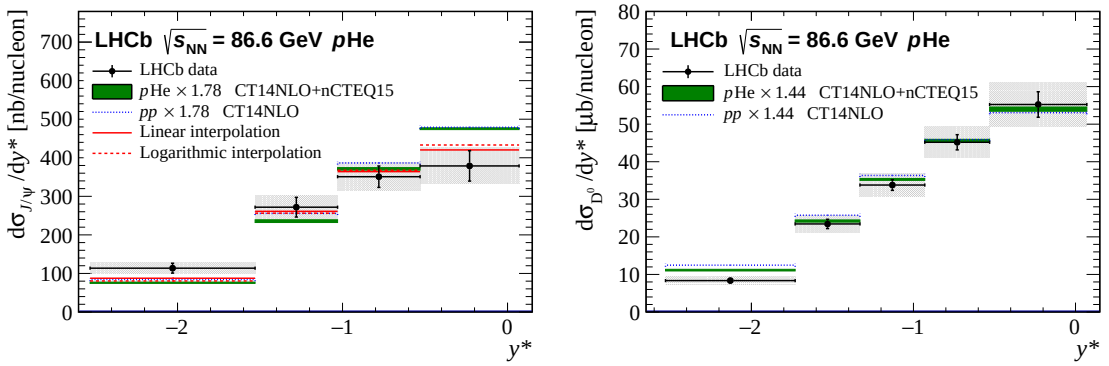

Figure 2: Differential J/ψ (left) and D^0 (right) production cross-sections for pHe collisions, as a function of centre-of-mass rapidity y^*. The data points mark the bin centres. The quadratic sum of statistical and uncorrelated systematic uncertainties are indicated by the vertical black lines. The correlated systematic uncertainties are indicated by the grey area.

LHCb has reported the first measurements of heavy-flavor production with its fixed-target mode [5]. J/ψ and D^0 production cross-sections and yields have been respectively measured in pHe collisions at $\sqrt{s_{NN}} = 86.6$ GeV and pAr collisions at $\sqrt{s_{NN}} = 110.4$ GeV, in the rapidity range $2 < y < 4.6$. In order to benefit from the detector performance and from calibration samples collected in pp collisions for data-driven determinations of the detector efficiencies, events are selected with a longitudinal position of the primary vertex between -200 and 200 mm with respect to the nominal interaction point. To suppress residual pp collisions, events with activity in the backward region are vetoed. The $J/\psi \to \mu^+\mu^-$ and $D^0 \to K^\pm\pi^\mp$ yields are obtained from an

extended unbinned maximum likelihood fits on their mass distributions. The cross-section measurement is made for the pHe sample only, since the luminosity determination is only available for this sample. It is determined from the yield of electrons elastically scattering off the target He atoms [6]. After correction for the acceptance, efficiencies and the branching fractions, the cross-sections are extrapolated to the full phase space, and the D^0 measurement is used to extract the $c\bar{c}$ cross-sections. These J/ψ and $c\bar{c}$ measurements are compared in Fig.1 with different centre-of-mass energy measurements by other experiments. The J/ψ and D^0 differential cross-sections per target nucleons obtained for the pHe dataset as function of the rapidity in the centre-of-mass (y^*) are shown in Fig. 2 with different predictions. In this specific phase space, any substantial intrinsic charm contribution should be seen in the pHe results. No strong differences are observed between the pHe data and the theoretical predictions which do not include any intrinsic charm contribution. Therefore, within uncertainties, no evidence of substantial intrinsic charm content of the nucleons is observed in the data. This analysis is a starting point for more detailed heavy-flavor fixed-target studies, including samples with high statistics such as pNe collisions collected in 2017.

4. Charmonium and open charm results with pPb collisions

The LHCb experiment has collected data of proton-lead collisions at $\sqrt{s_{NN}} = 5$ TeV in 2013 and 8.16 TeV in 2016. The 2013 data sample corresponds to an integrated luminosity of 1.06 ± 0.02 nb^{-1} for the forward region and 0.52 ± 0.01 nb^{-1} for the backward region, while the 2016 data corresponds to 13.6 ± 0.3 nb^{-1} for the forward region and 20.8 ± 0.5 nb^{-1} for the backward region. These data samples are used to measure the quarkonium and open charm or beauty production.

LHCb has measured the J/ψ production in both data samples [7]. Prompt J/ψ and non-prompt J/ψ -from-b-hadron decays are identified with the pseudo-proper decay time. The cross-sections are compared with the ones from the inter/extrapolated pp reference cross-sections with the nuclear modification factors, defined by

$$R_{pPb}(y^*, p_T) = \frac{1}{A} \frac{\mathrm{d}\sigma_{pPb}(y^*, (p_T))}{\mathrm{d}y^*(p_T)} / \frac{\mathrm{d}\sigma_{pp}(y^*, (p_T))}{\mathrm{d}y^*(p_T)}, \tag{4.1}$$

where A is the atomic mass number of the lead nucleus. Any deviation from unity of this factor indicates a relative enhancement (> 1) or suppression (< 1) of the pPb cross-section with respect to pp. The deviations from unity of the R_{pPb}, specially in the forward region and the low p_T region highlight the effect of the nuclear environment, as shown in Fig. 3 for prompt J/ψ and non-prompt J/ψ. At forward rapidity, a suppression up to 50% is observed for prompt J/ψ, at low transverse momentum. At backward rapidity, a weaker suppression of prompt J/ψ is observed. The production of J/ψ from-b-hadrons is also suppressed compared to pp collisions, but at a lower scale. Different theoretical predictions are in good agreement with the LHCb measurements (see details in [7]).

Using 2013 proton-lead collisions, LHCb measured the D^0 production cross-section [8]. The $D^0 \to K^-\pi^+$ analysis exploits the impact parameter significance of the D^0 to identify prompt D^0 from D^0 from b-hadron-decays. This feature, down to zero p_T region is unique to LHCb. D^0 yields are extracted by fitting the invariant mass distribution. The D^0 single-differential cross-sections and nuclear modification factors have been measured. As shown in Fig 4, R_{pPb} is above unity in

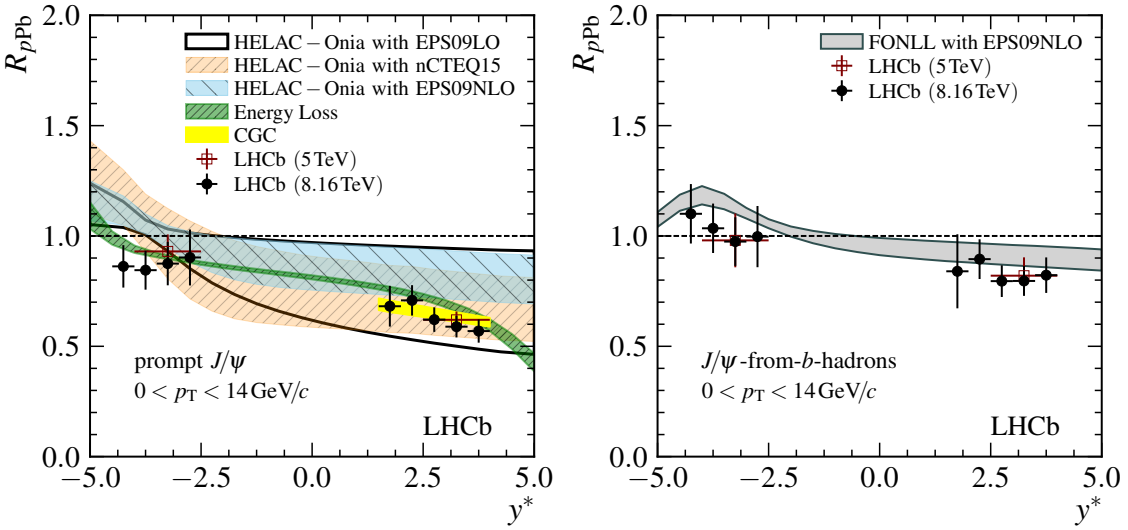

Figure 3: J/ψ nuclear modification factor, R_{pPb}, integrated over p_T in the range $0 < p_T < 14$ GeV/c, as a function of y for (left) prompt J/ψ and (right) J/ψ -from-b-hadron decays. The horizontal error bars are the bin widths and vertical error bars the total uncertainties. The black circles are the values measured at $\sqrt{s_{NN}} = 8.16$ TeV, the red squares the values measured at $\sqrt{s_{NN}} = 5$ TeV and the coloured areas the theoretical computations, with their uncertainties.

the backward region, while there is a strong suppression in the forward region. The D^0 and J/ψ cross-sections are also compared Fig 4, and no rapidity dependency is observed.

The same dataset and procedure are used to study Λ_c^+ production [9]. The cross-section ratio between Λ_c^+ baryon and D^0 mesons, providing information on the hadronisation mechanism in the charm sector, is shown in Fig 5. The theoretical predictions tuned to pp data indicate a slight increase with p_T and are consistent with data within the experimental uncertainties, except for the forward configuration in the high p_T region, where they overestimate the data.

5. Bottomium and open beauty results with pPb collisions

The 2016 proton-lead collisions are used to study the $\Upsilon(nS)$ mesons production [10], through their decays into two opposite-sign muons. The measurements comprise the differential production cross-sections of the $\Upsilon(1S)$ and $\Upsilon(2S)$ states and nuclear modification factors, performed as a function of the transverse momentum and rapidity in the nucleon-nucleon centre-of-mass frame of the $\Upsilon(nS)$ states. The three states are well-identified in pPb and Pbp configurations as shown in Fig. 6. Their nuclear modification factors are compared with theoretical predictions in Fig. 7, where suppressions for bottomium in pPb collisions are observed.

Nuclear effects in 2016 proton-lead data are also probed by double-differential cross-sections, forward-to-backward cross-section ratios and nuclear modification factors of the beauty hadrons [11]. The B^+, B^0, Λ_b are reconstructed through their decays $B^+ \to D^0\pi^+$, $B^+ \to J/\psi K^+$, $B^0 \to D^-\pi^+$ and $\Lambda_b^0 \to \Lambda_c^+\pi^-$. The double-differential cross-sections are measured as function of the beauty hadron transverse momentum and rapidity in the nucleon-nucleon centre-of mass frame. The nu-

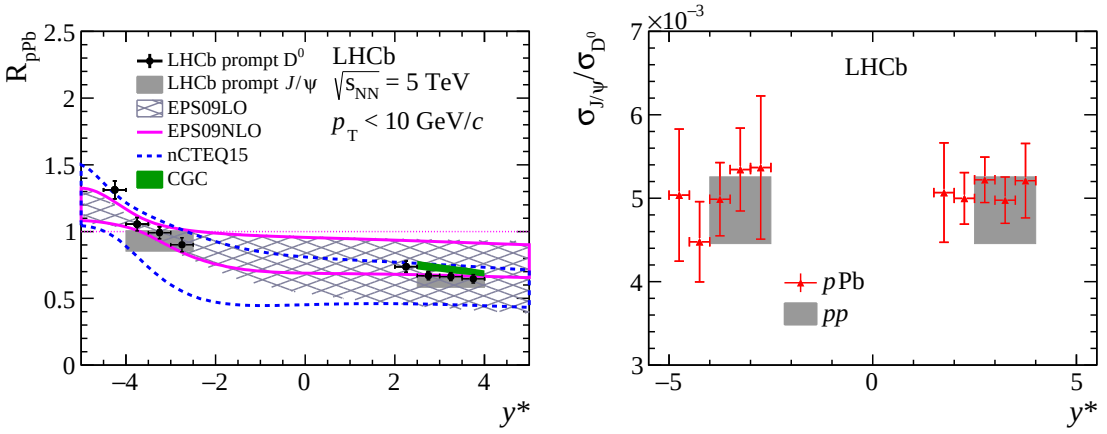

Figure 4: Left: nuclear modification factor R_{pPb} as a function of y for prompt D^0 meson production, integrated up to $p_T = 10$ GeV$/c$. The uncertainty is the quadratic sum of the statistical and systematic components. More details in [8].

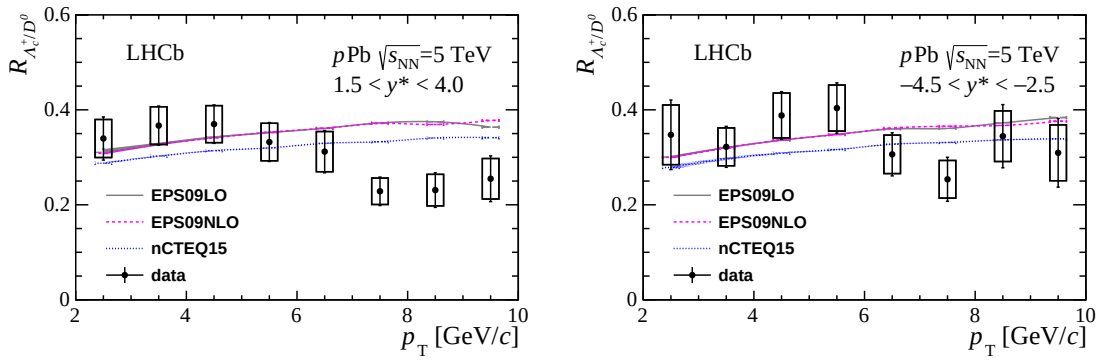

Figure 5: The cross-section ratio $R_{\Lambda_c^+/D^0}$ between Λ_c^+ baryons and D^0 mesons as a function of p_T integrated over four different rapidity regions. The uncertainty represents the sum in quadrature of the statistical and the systematic uncertainties. The coloured curves represent HELAC-Onia calculations with nPDF EPS09LO/NLO and nCTEQ15. More details in [9].

clear modification factors, shown in Fig. 8 for B^+, indicate a significant nuclear suppression at positive rapidity compared to pp collisions and compared to negative rapidity.

6. J/ψ production in ultra-peripheral PbPb collisions

Physics analyses of lead-lead collisions are limited to the 50% less central collisions due to saturation in LHCb detector. However there are still many opportunities to exploit PbPb collisions, specially in ultra-peripheral collisions, for which the impact parameter is greater than two times the nucleus radius. LHCb has measured the coherent production of J/ψ mesons in PbPb collisions at a nucleon-nucleon centre-of-mass energy of 5 TeV [12]. The J/ψ mesons, reconstructed in the dimuon final state, are required to have transverse momentum $p_T < 1$ GeV and rapidity $2.0 <$

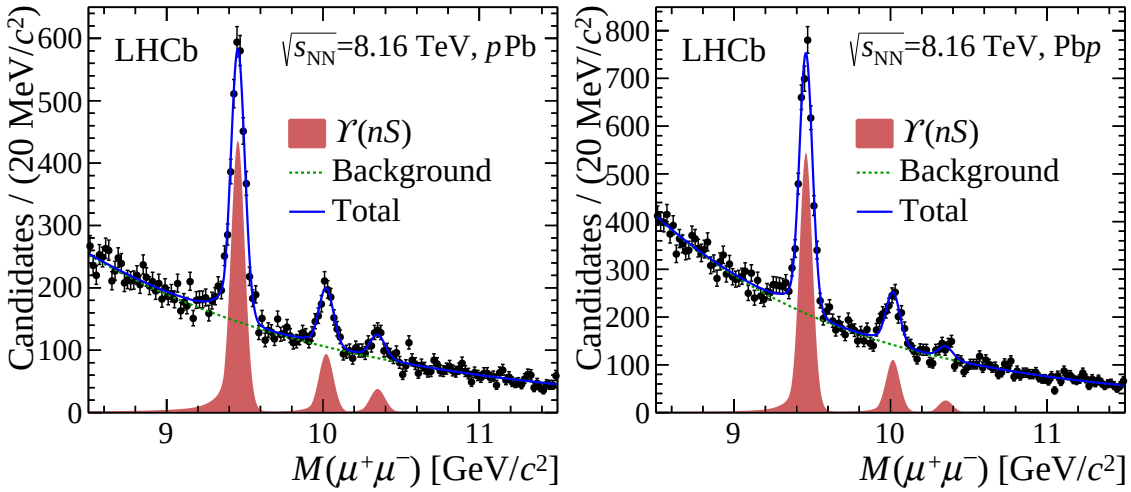

Figure 6: Invariant-mass distribution of $\mu^+\mu^-$ pairs from the (left) pPb and (right) Pbp samples after the trigger and offline selections.

$y < 4.5$. The event activity is controlled by applying vetoes on the number of tracks and the energy deposit in the calorimeter. The dimuon invariant mass is shown in Fig. 9. The cross-section within this fiducial region is measured to be $\sigma = 5.3 \pm 0.2(stat) \pm 0.5(syst) \pm 0.7(lumi)$ mb. The differential cross-section, measured in five bins of J/ψ rapidity, is compared to predictions from phenomenological models in Fig. 9. Data are well reproduced by model predictions within uncertainty except for one model that includes sub-nucleonic fluctuations.

7. Conclusions

The LHCb detector has measured the heavy-quark production in proton-nucleus and lead-lead collisions. These measurements improve the understanding of cold nuclear matter effects down to low p_T. Thanks to the excellent performance of the LHC and LHCb, there are many recent data samples to analyze: 2018 lead-lead collisions whose integrated luminosity overtake previous PbPb collisions by at least a factor 20, the proton-neon collisions collected in 2017 which correspond to the largest fixed-target data sample, and the first high-statistics lead-induced collisions in the fixed-target configuration.

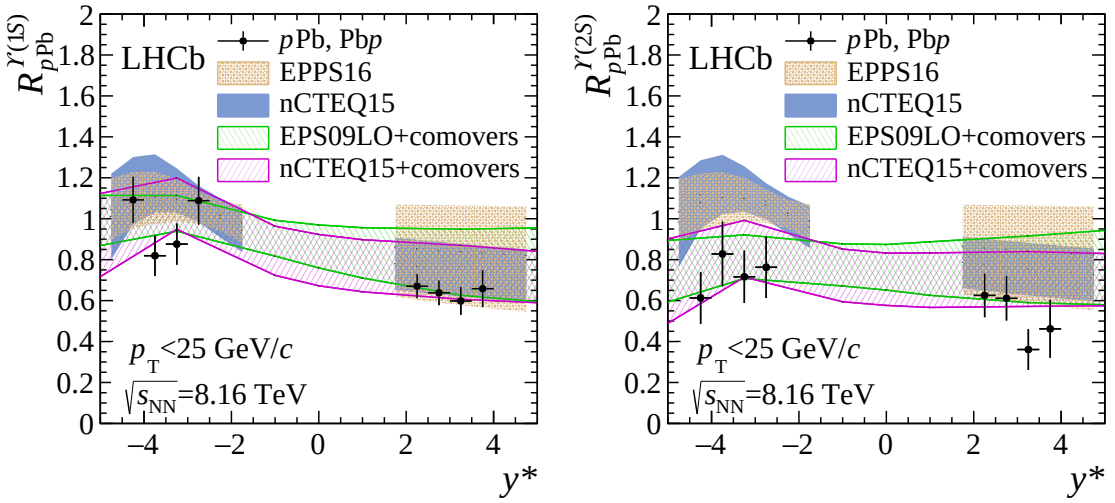

Figure 7: Nuclear modification factors of the (left) $\Upsilon(1S)$ and (right) $\Upsilon(2S)$ mesons as a function of y integrated over p_T for the forward and backward samples. The bands correspond to the theoretical predictions for the nCTEQ15 and EPPS16 NNPDF sets, and the comovers model.

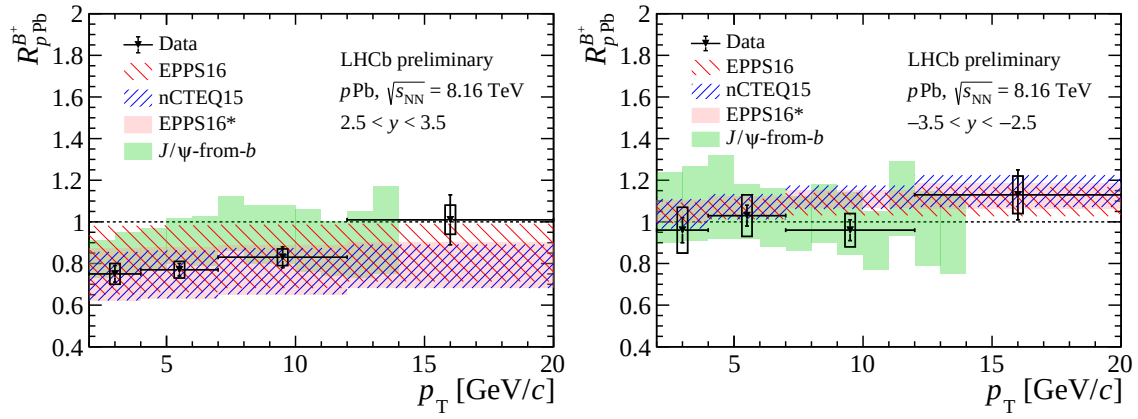

Figure 8: R_{pPb} of B^+ mesons as function of (top) y and as function of p_T in (bottom left) pPb and (bottom right) Pbp compared with HELAC-onia calculations using different nPDF sets as well as with the measurement of non-prompt J/ψ R_{pPb}. For the data points, the bars (boxes) represent the statistical (systematic) uncertainties. More details in [11].

References

[1] R. Aaij *et al.* [LHCb Collaboration], "LHCb Detector Performance", Int. J. Mod. Phys. A **30** (2015) no.07, 1530022 doi:10.1142/S0217751X15300227 arXiv:1412.6352 [hep-ex]

[2] R. Aaij *et al.* [LHCb Collaboration], "Precision luminosity measurements at LHCb", JINST **9** (2014) P12005, arXiv:1410.0149 [hep-ex]

[3] T. Matsui and H. Satz, Phys. Lett. **B178** (1986) 416

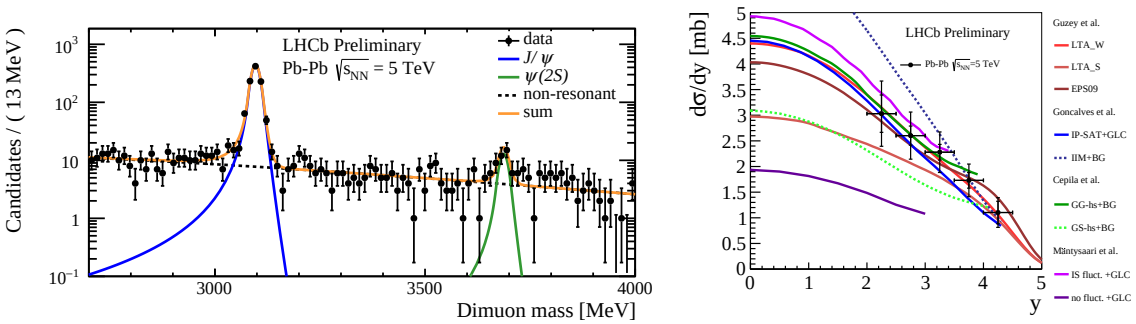

Figure 9: Left: dimuon invariant mass spectrum in the range between 2.7 and 4.0 GeV. The contribution of (solid blue line) J/ψ , (solid green line) $\psi(2S)$ and (black dashed line) non resonant are shown individually and the sum of all contributions is represented by the orange curve. Right: differential cross-section for coherent J/ψ production compared to different phenomenological predictions. The LHCb measurements are shown as points, where inner and outer error bars represent the statistical and the total uncertainties respectively.

[4] P. Braun-Munzinger and J. Stachel, Phys. Lett. **B490** (2000) 196

[5] R. Aaij *et al.* [LHCb Collaboration], "First measurements of charm production in fixed-target configuration at the LHC", Submitted to PRL, (2018) arXiv:1810.07907 [hep-ex]

[6] R. Aaij *et al.* [LHCb Collaboration], "Measurement of antiproton production in pHe collisions at $\sqrt{s_{\rm NN}} = 110$ GeV, LHCb-PAPER-2018-031 to be published, arXiv:1808.06127

[7] R. Aaij *et al.* [LHCb Collaboration], "Prompt and nonprompt J/ψ production and nuclear modification in pPb collisions at $\sqrt{s_{\rm NN}} = 8.16$ TeV", Phys. Lett. **B774** (2017) 159, arXiv:1706.07122

[8] R. Aaij *et al.* [LHCb Collaboration], "Study of prompt D^0 meson production in pPb collisions at $\sqrt{s_{\rm NN}} = 5$ TeV", JHEP **1710** (2017) 090 doi:10.1007/PhysRevLett.111.222.301 arXiv:1707.02750 [hep-ex]

[9] R. Aaij *et al.* [LHCb Collaboration], "Prompt Λ_c^+ production in pPb collisions at $\sqrt{s} = 5.02$ TeVâĂİ, Submitted to JHEP (2018) arXiv:1809.01404 [hep-ex]

[10] R. Aaij *et al.* [LHCb Collaboration], "Study of Υ production in pPb collisions at $\sqrt{s_{\rm NN}} = 8.16$ TeV, arXiv:1810.07655 .

[11] R. Aaij *et al.* [LHCb Collaboration], B^+, B^0 and λ_b^0 production and nuclear modification in pPb collisions at $\sqrt{s_{\rm NN}} = 8.16$ TeV, LHCb-CONF-2018-004

[12] R. Aaij *et al.* [LHCb Collaboration], "Study of coherent J/ψ production in lead-lead collisions at $\sqrt{s_{\rm NN}} = 5$ TeV with the LHCb experiment", LHCb-CONF-2018-003